ADVANCED MATERIALS

DOI: 10.1002/adma.200800395

Exploration of a Standing Mesochannel System with Antimatter/Matter Atomic Probes**

By *Hiroyuki K. M. Tanaka,* Yusuke Yamauchi, Toshikazu Kurihara, Yoshio Sakka, Kazuyuki Kuroda,* and *Allen P. Mills Jr.*

Since the discovery of mesoporous materials through the self-organization of surfactants,[1–4] a huge number of mesoporous materials with various morphologies including powders, monoliths, spheres, rods, fibers, and films have been reported. Continuous mesoporous silica films with high transparency, regularly ordered mesoporous structures, and high surface areas have attracted broad interest because of their wide applicability in optics and electronics.[5–9] Controlling the alignment of mesochannels in 2D hexagonally ordered mesoporous films is of technological interest because of their applications ranging from ultrahigh-density magnetic recording media to sensitive gas sensors and separation technologies. This attractive pore system can be used as next-generation hosts for numerous molecular and cluster-based catalysts,[10] for selective sequestration of contaminants[11] and chromatography,[12] for the stabilization of conducting nanoscale wires,[13–15] as a matrix for carbon casting,[16] and for novel drug-delivery systems.[17,18] The transport of guest molecules in the channels is of importance for successful preparation or for the functionality of the materials. However, no techniques have been available to track the particle trajectories inside such standing mesochannel systems. A recently developed new technique using molecular probes[19] cannot address this problem because it only gives horizontal information.

Mesoporous structures are commonly characterized with X-ray diffraction,[20–22] electron microscopy methods,[23,24] gas sorption techniques,[25] pulsed-field gradient NMR spectroscopy,[26] and neutron scattering.[27] Fluorescence correlation spectroscopy was recently applied to study diffusion in mesoporous films,[19] and individual trajectories were obtained. However, this technique only gives information on the particle trajectories parallel to the film substrate. On the other hand, a quantitative measurement of the accessibility towards the outside of a recently developed magnetically induced standing 2D hexagonal mesoporous film would provide important information on the fabrication of a patterned recording medium, which would be a promising candidate for the next generation of perpendicular recording media beyond 1 Tbit $inch^{-2}$, highly sensitive chemical sensors, and separation membranes for molecules that are too large to process with crystalline zeolite molecular sieves.

In this paper, depth-profiled positronium time-of-flight (Ps-TOF) spectroscopy[28–30] serves to provide the accessibility of standing 2D hexagonal mesoporous film for the first time. Such mesochannels form a passage allowing positronium atoms (Fig. 1d) to diffuse and escape into vacuum. Ps-TOF measures the time between when Ps was generated in the mesoporous silica and when Ps escaped from the surface of the film. The results give a detailed picture of the structure and connectivity for different depths and different mesopore systems. Similar to a molecular technique developed by

[*] Prof. H. K. M. Tanaka
Earthquake Research Institute, University of Tokyo
1-1-1 Yayoi, Bunkyo-ku, Tokyo 113-0032 (Japan)
E-mail: ht@riken.jp
Prof. H. K. M. Tanaka, Prof. A. P. Mills
Physics Department, University of California
Riverside CA 92521 (USA)
Prof. H. K. M. Tanaka
Atomic Physics Laboratory, RIKEN
2-1 Hirosawa, Wako-shi, Saitama 351-0198 (Japan)
Prof. Y. Yamauchi, Y. Sakka
World Premier International (WPI) Research Center
International Center for Materials Nanoarchitectonics (MANA)
National Institute for Materials Science (NIMS)
1-1 Namiki, Tsukuba-shi, Ibaraki 305-0044 (Japan)
Prof. T. Kurihara
Slow Positron Facility, Institute of Materials Science Structure Science (IMSS)
High Energy Accelerator Research Organization (KEK)
1-1 Oho, Tsukuba-shi, Ibaraki 305-0801 (Japan)
Prof. Y. Sakka
Nanoceramics Center, National Institute for Materials Science (NIMS)
1-2-1 Sengen, Tsukuba-shi, Ibaraki 305-0047 (Japan)
Prof. K. Kuroda
Department of Applied Chemistry, Faculty of Advanced Science and Engineering
Waseda University
3-4-1 Ohkubo, Shinjuku-ku, Tokyo 169-8555 (Japan)
Prof. K. Kuroda
Kagami Memorial Laboratory for Materials Science and Technology, Waseda University
2-8-26 Nishi-Waseda, Shinjuku-ku, Tokyo 169-0051 (Japan)

[**] The authors acknowledge Mr. M. Fuziwara (Kagami Memorial Laboratory for Materials Science and Technology, Waseda University) for preparation of TEM samples, and Mr. M. Sawada, Mr. M. Komatsu, and Mrs. A. Takai (Waseda University) for experimental support. The present study is supported by the Global COE Program ''Practical Chemical Wisdom'', and the Encouraging Development Strategic Research Centers Program (Super COE) ''Establishment of a Consolidated Research Institute for Advanced Science and Medical Care'' from the Japanese Ministry of Education, Culture, Sports, Science and Technology (MEXT). The present study is supported in part by the A3 Foresight Program ''Synthesis and Structural Resolution of Novel Mesoporous Materials'' from the Japan Society for the Promotion of Science (JSPS). This work was supported by a Grant-in-Aid for Scientific Research (No. 19850031) from JSPS.

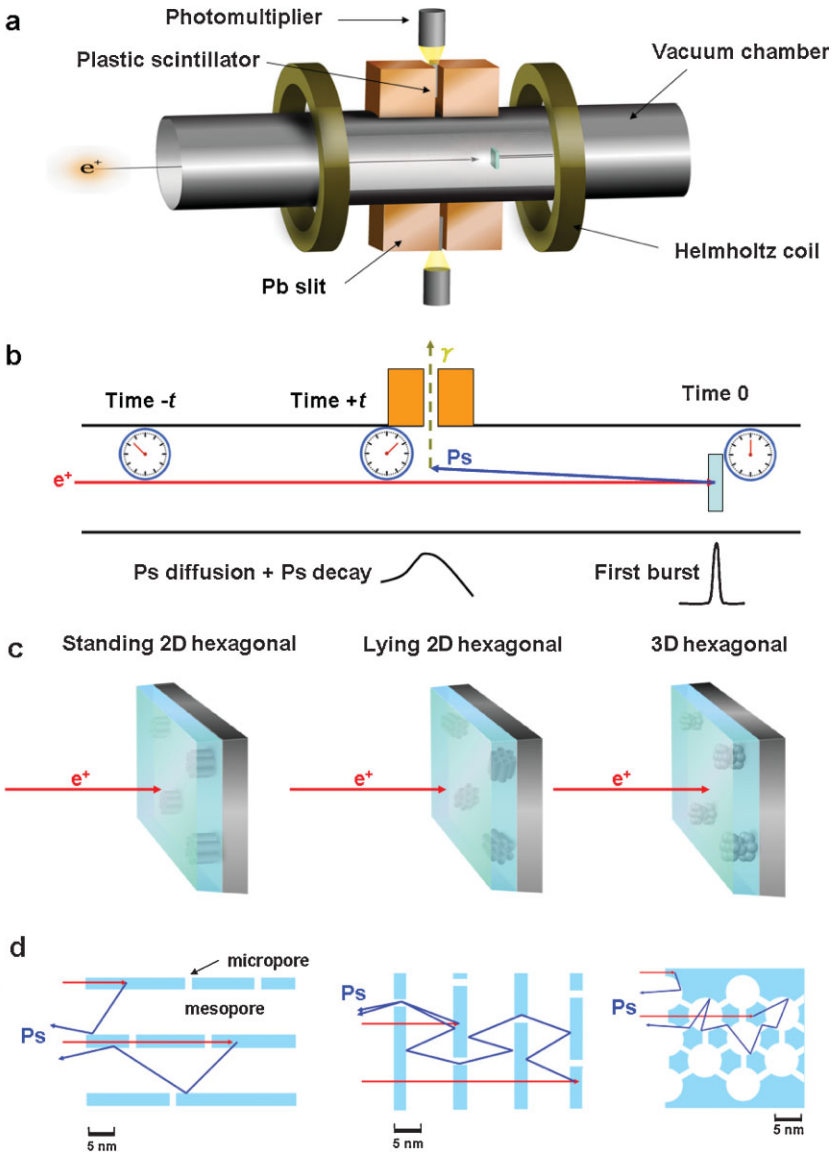

Figure 1. a) Schematic layout of the experimental setup. b) The principle of Ps-TOF measurement. c) The conceptual view of three different mesoporous films: standing 2D hexagonal, lying 2D hexagonal, and 3D hexagonal mesoporous films. d) The conceptual view of depth profiling and Ps diffusion in three different mesoporous films: standing 2D hexagonal, lying 2D hexagonal, and 3D hexagonal mesoporous films.

Kirstein et al.,[19] Ps atoms directly leave the inner pore system of the host. An advantage of this technique — contrary to the molecular technique — is that vertical accessibility of the pore system can be obtained by tracking Ps atoms that diffuse out of the sample. This is difficult to measure with the molecular technique because the thickness of the sample, which is usually hundreds of monometers, is too thin to track single molecules by fluorescence microscopy techniques. Positronium annihilation lifetime spectroscopy (PALS)[31–35] has been widely applied to study mesoporous silica. However, the use of the lifetime of positronium can be limited for measuring the pore size and it is therefore difficult to establish pore connectivity and accessibility.

The mesoporous silica film with perpendicular mesochannels was prepared by applying a magnetic field of 12 T (Fig. 2).[36] The conventional θ–2θ X-ray diffraction (XRD) profile of the mesoporous silica film shows one broad peak,[36] while that of a mesoporous silica film without a magnetic field shows two peaks corresponding to (10) and (20) diffractions of ordered 2D-hexagonal structure (Fig. 2d). The intensity of (10) diffraction is decreased dramatically by applying a high magnetic field. With θ–2θ XRD measurements, only structural information parallel to substrate can be obtained.[37] Therefore, the intensity decrease strongly suggests that the orientation of the mesochannels in the film was induced along the direction perpendicular to the substrate. In some domains, mesochannels were inclined at about 40°–70° to the substrate, while the mesochannels were aligned completely perpendicularly to the substrate in other domains of the inner parts of the film (Fig. 2e). The mesostructure of this sample has already been confirmed by cross-sectional transmission electron microscopy (TEM) images in our previous study.[38] Figure 2f shows a top-surface scanning electron microscopy (SEM) image of the mesoporous silica film without magnetic field. All the 2D mesochannels are oriented parallel to the surface of the film, showing several types of morphologies, such as S-, Y-, and swirl-shapes.[39] Note that it is difficult to judge the true size of the domains of mesoporous crystals in lying 2D hexagonal mesoporous film. Furthermore, TEM and SEM images give no information about the real connectivity of the pores for molecules diffusing in them. A nitrogen adsorption-desorption isotherm of the calcined film synthesized under 12 T was characteristic of mesoporous materials. The Brunauer-Emmett-Teller (BET) surface area was about 840 m^2 g^{-1}. The presence of both mesopores (9.0 nm) and micropores (below 3 nm) was observable. The density was 0.62 g cm^{-3}. These values were similar to those of the film synthesized under 0 or 12 T, which is the same phenomenon as the CTAB system.[40] Such microporosity has been observed for mesoporous materials prepared by block-copolymers such as P123,[41] and thus provide the space for Ps (0.5 nm in diameter) molecular movement. The 3D hexagonal mesoporous film was prepared by spin-coating according to a previous study.[38] The diameter of spherical mesopores and the BET surface

ADVANCED MATERIALS

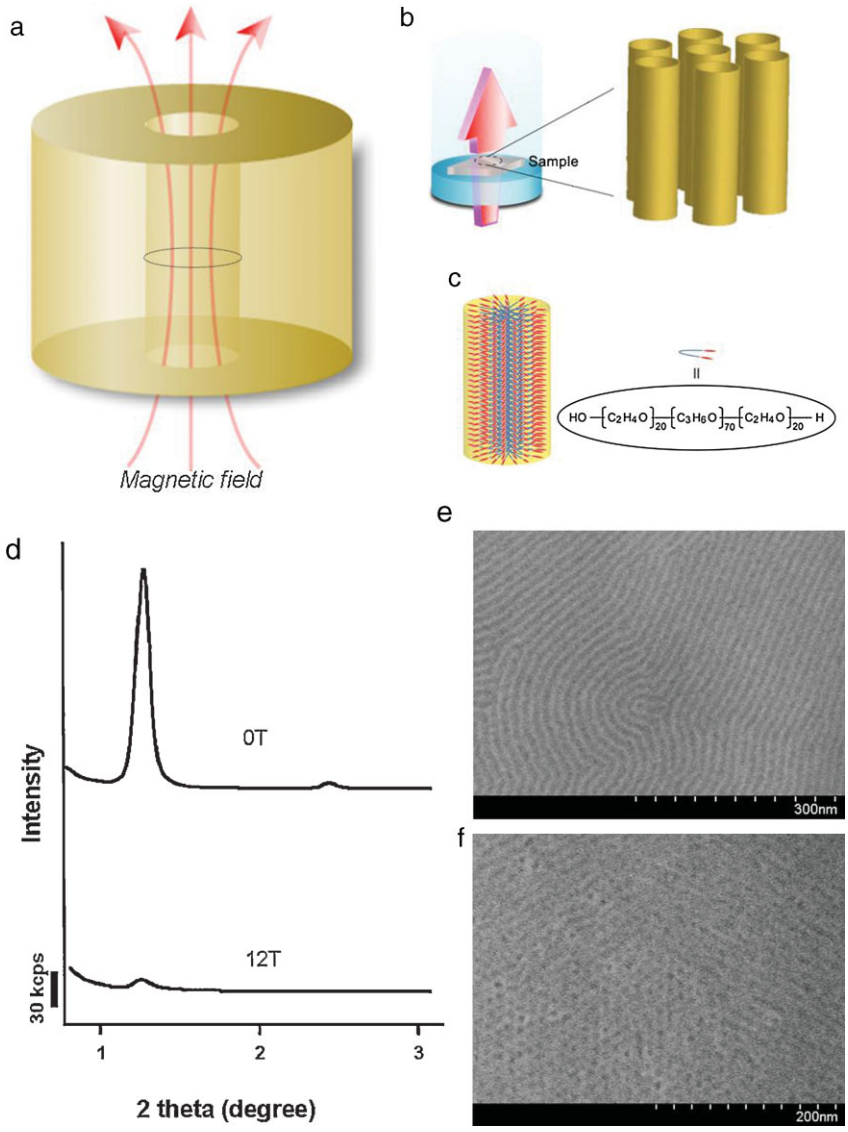

Figure 2. a) Schematic view of the experimental setup of preparation of mesoporous silica films under a magnetic field of 12 T which is generated by a hybrid magnet. b) The enlarged image near the film. c) The chemical structure of the surfactant. d) θ–2θ scanning XRD profiles of the calcined films synthesized under 0 (top) and 12 Tesla (bottom). Top-surface SEM image of the calcined film synthesized under 0 T (e) and 12 T (f).

area are 5.4 nm and 523 $m^2\ g^{-1}$, respectively. The density was 1.13 g cm^{-3}.

The Ps-TOF was measured at the Slow Positron Facility, High Energy Accelerator Research Organization.[42] The facility consists of a 50 MeV linac, an assembly of slow positron generator, a slow positron transport line, and an experimental station. For the TOF measurements, the sample is bombarded with a slow positron beam (Fig. 1a). The time interval between the linac signal and the detection of the gamma ray from the emitted Ps self-annihilation is measured. In the present experiment, a lead collimator was placed to reduce the annihilation gamma rays from the sample region to detect only the decay events from self-annihilation of Ps in the view of the scintillation counters through a 4.5 mm lead slit, as shown in Figure 1b. Ps-TOF accurately provides the time between when Ps is generated in the porous silica and when Ps escapes from the surface of the sample and arrives at the position of the slit (Fig. 1b) by measuring the time between the initial burst (a sum of fast Ps decay events) and o-Ps decay events. If the o-Ps diffusion time is longer than its lifetime of 10–100 ns (depending on the diameter of the mesochannels), it decays in the sample and cannot be detected by the counters. Beam-based Ps-TOF possesses the particular advantage of being capable of depth-profiling very thin films. The positron-implantation depth can be controlled precisely to a resolution of up to 10 nm by changing the positron implantation energy. We used depth-profiled Ps-TOF spectroscopy to explore the vertical accessibility and connectivity of standing and lying 2D hexagonal mesochannel systems of the mesoporous silica film in comparison reference to that of a 3D hexagonal system (Fig. 1c and 1d).

We performed a Ps-TOF measurement experiment at the downstream end of the beam line. The pulse heights, the annihilation gamma rays, and the time when annihilation events occur are recorded by a digital oscilloscope (LeCroy Wavepro 960). A pulse fed from the linac triggered the start. The scintillator was 600 mm in diameter and 10 mm thick and was coupled on opposite sides to a photomultiplier tube (HAMAMATSU H 1949) through a Lucite light guide (Fig. 1a). The vacuum level in the sample chamber was kept at 10^{-8}–10^{-9} Torr (1 Torr = 133 Pa) throughout the experiment. The sample bias can be varied in the range of 0–9 keV by changing the electric potential of the sample by using a retarding element (RET). The energy of the slow positron beam is 5 keV. The beam size was 1 cm in diameter. The beam intensity and the pulse width were 2×10^5 positrons/pulse and 22 ns, respectively.

Figure 3a shows the Ps-TOF spectrum of the lying 2D hexagonal mesoporous film for the sample position, $z = 0$ mm (the distance between the slit and the sample position). In this case, we directly observe o-Ps annihilations in the pores. The spectrum curve will have a characteristic lifetime, which is the same as the lifetime of the Ps in the pores. This turns out to be 106 ns, which is exactly the same value as found in previous measurements on porous materials of similar characteristics, i.e., having 9 nm pores.[43] Figure 3b shows the Ps-TOF

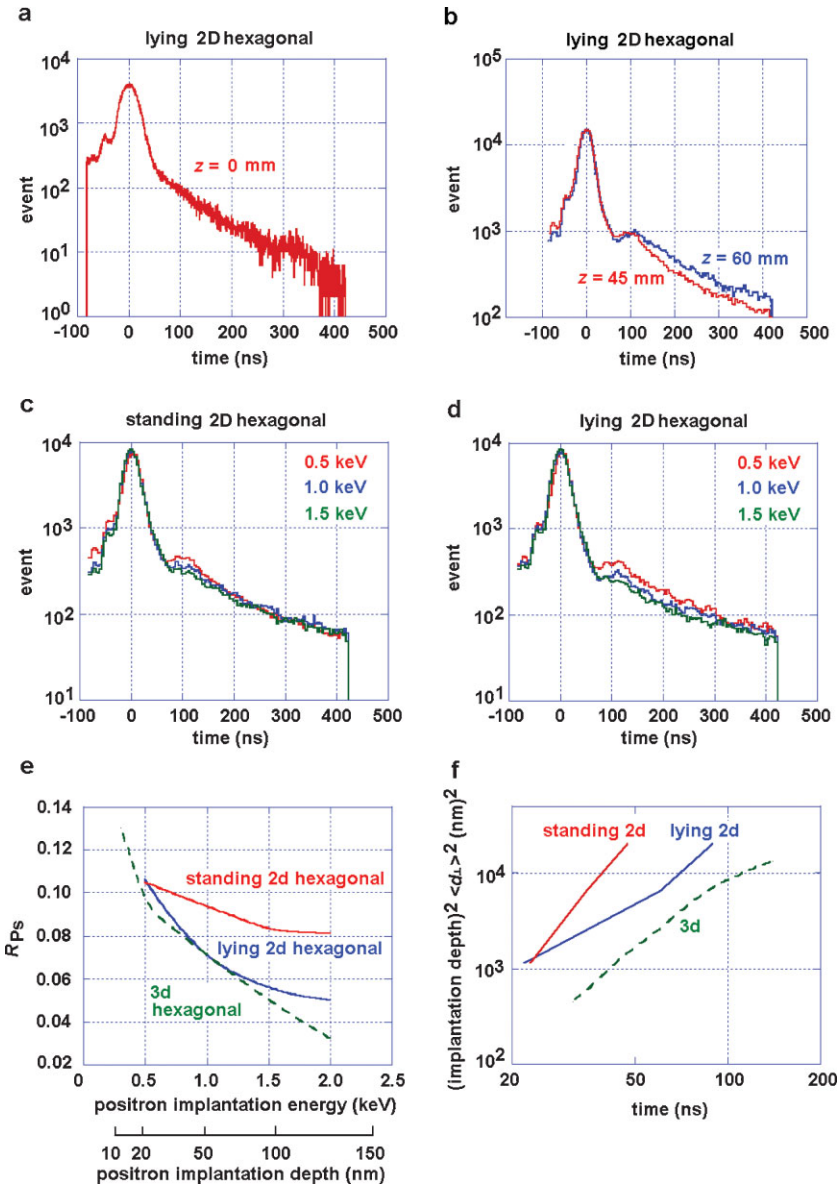

Figure 3. a) Ps-TOF spectrum from the lying 2D hexagonal mesoporous film for the sample position, $z = 0$ mm (the distance between the slit and the sample position). The time t was set to zero at the early peak. The counts for $t < 0$ are associated with gamma rays and neutrons from the bremsstrahlung pair production target. b) The Ps-TOF spectrum for the different sample positions, $z = 45$ mm and $z = 60$ mm. Ps-TOF spectra for various positron impact energies, 0.5 keV, 1.0 keV, and 1.5 keV for c) standing and d) lying 2D hexagonal films, respectively. The distance between the sample and the detector slit is 45 mm. e) A ratio of the Ps yield from the samples to total decay events as a function of the positron implantation depth. f) Double logarithmic plots of the mean square vertical displacement $\langle d_{\perp}^2 \rangle$ versus Ps diffusion time t.

spectrum for the different sample positions, $z = 45$ mm and $z = 60$ mm. The positron impact energy is 500 eV. All the data were normalized to the event number (100 000 events). The early peak in Figure 3 is a sum of fast Ps decay events, which essentially represents the time when Ps atoms are produced in the film. The width of the peak is determined by the linac pulse width. This peak does not provide information on the nanoporous structure and is neglected in the following discussion. The time was set to zero at the maximum of this peak. When the positrons are implanted into the mesoporous film using an implantation energy of 500 eV, they find themselves in porous silica, which forms positronium efficiently. This Ps will essentially be emitted instantaneously compared to the relevant times of flight, which are 90 ns for $z = 45$ mm and 105 ns for $z = 60$ mm, thus leading to the small delayed peak at the position of the vertical bar in Figure 3b. We can assume that the pores at the surface of the film are half opened (Fig. 1d). This is easily understood, because the velocity of the emitted positronium, 15 mm/15 ns = 10^8 cm s^{-1} ($E_{Ps} = 3$ eV) is characteristic of the Ps negative affinity for amorphous silica as reported by Sferlazzo et al.[44]

Figure 3c and 3d show the Ps-TOF spectra for various positron impact energies, 0.5 keV, 1.0 keV, and 1.5 keV for standing and lying 2D hexagonal films, respectively. The distance between the sample and the detector slit is 45 mm. Figure 3e shows the ratio of the Ps yield from the samples to total decay events as a function of positron implantation depth. This plot was extracted from Figure 3c and 3d. The ratio was calculated by $R_{Ps} = (N_{Ps150–500\,ns} - k)/(N_{Ps} - k)$, where N_{Ps} is the number of total decay events, $N_{Ps150–500\,ns}$ the number of decay events integrated over the region from 150 ns to 500 ns, and k a background constant. The variations in Ps yield reflect the sample structure. As shown in Figure 3e, at 0.5 keV, the fractions of the Ps yield from 2D and 3D hexagonal films are almost the same. This is probably because the first layer of mesopores at the top surface is open on all samples (Fig. 1d), as confirmed by high-resolution scanning electron microscopy (HR-SEM). Above 1 keV the Ps forms copiously in the mesopores and escapes through either mesopores or micropores in the pore walls. Our picture is as follows: a) in the standing 2D hexagonal mesoporous film, Ps escapes mostly through mesopores, and b) in the lying 2D and 3D hexagonal samples Ps escapes through micropores. However, the micropores themselves do not lead to significant Ps emission at higher implantation energies because the micropore density is low, leading to a large difference in the Ps emission rate between standing and lying 2D mesochannel systems.

The different diffusive behavior can also be visualized by plotting the mean square vertical displacement $\langle d_{\perp}^2 \rangle$ of the Ps atoms as a function of Ps diffusion time t (Fig. 3f).[45] The

ADVANCED MATERIALS

vertical displacement $d_{\perp}$ was computed from the positron stopping power and the density of the sample (0.62 g cm^{-3} for the 2D hexagonal and 1.13 g cm^{-3} for the 3D hexagonal sample). The Ps diffusion time is defined as $-\ln(F_{Ps} \times \tau)$, where F_{Ps} is the fraction of the Ps emitted from the sample surface and τ is the characteristic Ps lifetime. Assuming regular Brownian motion according to the Einstein-Smoluchowski relation, $\langle d^2 \rangle = 2\ nDt$[46], with $n = 1$, 2 or 3 corresponding to one-, two- or three-dimensional diffusion, respectively. The diffusion coefficient D can be extracted from the vertical intercepts of double logarithmic plots of $\langle d^2 \rangle$ versus t. Figure 3f (red and blue lines) shows clearly that a big difference exists between standing and lying 2D hexagonal mesoporous films. This can be explained by the difference in vertical accessibility of these films. The diffusion coefficients differ by an order of magnitude between two different alignments in mesochannel systems, standing and lying. A dark green dotted line (Fig. 3f) for the 3D hexagonal film is also shown. In a typical synthesis using P123 surfactant, hexagonal, cubic, and lamellar mesostructures are produced. In this study we investigated how the positronium time-of-flight spectrum is affected in different mesostructural phases. It is difficult for us to use a sample with a lamellar structure as a reference, because mesopores disappear when they are calcinated. Therefore, we used the cubic structure as reference. Because the pore/pore wall ratio in the 3D hexagonal film is smaller than that in the 2D hexagonal film, Ps diffuses slower in 3D hexagonal film than in 2D hexagonal film. An interesting observation for the 2D hexagonal mesochannel system is that the plots for this system are almost linear, while that for a 3D hexagonal system bends towards a horizontal asymptote as the implantation depth becomes deeper. A horizontal asymptote for a 3D hexagonal system is characteristic of diffusion in confined regions, which in our case are the domain explored by Ps. The domain size of this 3D hexagonal system, extracted from the horizontal asymptote is a few hundred nanometers, which is consistent with the size of the domain extracted from a direct HR-SEM observation of a 3D hexagonal film of similar characteristics.[35] On the other hand, the linear plots for 2D hexagonal films show that clear domains cannot be observed in 2D hexagonal samples. This domainless structure has also been confirmed by a direct HR-SEM observation of a 2D hexagonal film.[36] The diffusivities given above confirm that there are no clear domains in a magnetically induced standing 2D hexagonal mesochannel system.

We have shown how tracking Ps by Ps-TOF techniques can be used to study anisotropic mesoporous systems. We measured the Ps-TOF for several mesochannel systems with the standing and lying 2D hexagonal and 3D hexagonal systems in order to investigate the vertical connectivity and accessibility of the mesochannels to the outside, and we showed that the diffusion coefficient of the standing 2D hexagonal film is an order of magnitude bigger than the lying 2D and 3D hexagonal films. Whereas molecular probe methods are restricted to horizontal exploration parallel to the substrate, we can use depth-profiled Ps-TOF spectroscopy to investigate the vertical structure. These data provide direct information about nanometer-scale connectivity and accessibility of the channels, and the structural domains within the porous sample. We anticipate that standing 2D hexagonal mesochannel systems will become a candidate for next-generation host materials. The methodology for exploring the vertical structure of anisotropic mesochannel systems has been established. The method is also applicable to exploring nonartificial nanostructural materials, such as the nanostructure of terrestrial magmatic products or meteorites.

Experimental

Materials: Tetraethoxysilane ($(C_2H_5O)_4Si$, TEOS, purity >99.0%) as Si source was purchased from Kishida Chemical Co. Polyethylene oxide-polypropylene oxide-polyethylene oxide triblock copolymers of EO_{20}-PO_{70}-EO_{20} (Pluronic P123) was purchased from Aldrich Chemical Co. Ethanol (C_2H_5OH) and hydrochloric acid (HCl) were purchased from Junsei Chemical Co. and Kanto Chemical Co., respectively.

Preparation of Mesoporous Silica Films: The P123-based precursor solution was prepared according to previous reports [33] TEOS (5.2 g), ethanol (6 g), and diluted HCl (pH 2) solution (2.7 g) were mixed. After stirring for 20 min, P123 (1.38 g) and ethanol (4 g) were added and stirred for 3 h. Total molar ratio is 16.6 TEOS/0.158 P123/0.0180 HCl/145 C_2H_5OH/100 · H_2O. The precursor solution was cast onto a glass substrate. Then, the substrate was immediately put into the conductive magnet within a few seconds. The film was dried for 1 h at room temperature under high magnetic field (12 Tesla) perpendicular to the substrates. After drying, the as-prepared film was calcined at 400 °C for 4 h at the heating rate of 1 °C min^{-1}.

Characterization: The θ–2θ XRD profiles in the lower diffraction angles were measured by a Mac Science M03XHF22 diffractometer with Mn-filtered Fe Kα radiation (40 kV, 20 mA) at a scanning rate of 0.5° min^{-1}. The cross-sectional slices of film, less than 100 nm in thickness, were prepared by using an ultramicrotome. TEM images were acquired by a JEOL JEM-2010 transmission electron microscope using an accelerating voltage of 200 kV. The HR-SEM images without any metal coating were obtained with a Hitachi S-5500 scanning electron microscope using an accelerating voltage of 20 kV. Nitrogen adsorption and desorption isotherms were obtained using an Autosorb-1 instrument (Quantachrome Instruments, Inc) at 77 K. The calcined mesoporous silica film was heated at 120 °C for 3 h prior to measurement.

Received: February 8, 2008
Published online: October 22, 2008

[1] T. Yanagisawa, T. Shimizu, K. Kuroda, C. Kato, *Bull. Chem. Soc. Jpn.* **1990**, *63*, 988.
[2] T. Yanagisawa, T. Shimizu, K. Kuroda, C. Kato, *Bull. Chem. Soc. Jpn.* **1990**, *63*, 1535.
[3] C. T. Kresge, M.E. Leonowicz, W. J. Roth, J. C. Vartuli, J. S. Beck, *Nature* **1992**, *359*, 710.
[4] S. Inagaki, Y. Fukushima, K. Kuroda, *J. Chem. Soc. Chem. Commun.* **1993**, *680.*
[5] M. Ogawa, *J. Am. Chem. Soc.* **1994**, *116*, 7941.
[6] M. Ogawa, *Chem. Commun.* **1996**, *1149.*
[7] Y. F. Lu, R. Ganguli, C. D. Drewien, M. T. Anderson, C. J. Brinker, W. Gong, Y. Guo, H. Soyez, B. Dunn, M. H. Huang, J. I. Zink *Nature* **1997**, *389*, 364.

[8] T. Yui, T. Tsuchino, K. Akatsuka, A. Yamavchi, Y. Kobayashi, T. Hattori, M. Haga, K. Takagi *Bull. Chem. Soc. Jpn.* **2006**, *79*, 386.
[9] S. Tanaka, H. W. Hillhouse, *Chem. Lett.* **2006**, *928.*
[10] D. E. De Vos, M. Dams, B. F. Sels, P. A. Jacobs, *Chem. Rev.* **2002**, *102*, 3615.
[11] S. J. L. Billinge, E.J. Mckimmey, M. Shatnawi, H. J. Kim, V. Petkov, D. Wermeille, T. J. Pinnavaia *J. Am. Chem. Soc.* **2005**, *127*, 8492.
[12] V. Rebbin, R. Schmidt, M. Fröba, *Angew. Chem. Int. Ed.* **2006**, *45*, 5210.
[13] D. J. Cott, N. Petkov, M. A. Morris, B. Platschek, T. Bein, J. D. Holmes *J. Am. Chem. Soc.* **2006**, *128*, 3920.
[14] B. Ye, M. L. Trudeau, D. M. Antonelli, *Adv. Mater.* **2001**, *13*, 561.
[15] N. Petkov, N. Stock, T. Bein, *J. Phys. Chem. B* **2005**, *109*, 10737.
[16] R. Ryoo, S. H. Joo, M. Kruk, M. Jaroniec, *Adv. Mater.* **2001**, *13*, 677.
[17] C.-Y. Lai, B. G. Trewyn, D. M. Jeftinija, K. Jeftinija, S. Xu, S. Jeftinija, V. S. Y. Lin *J. Am. Chem. Soc.* **2003**, *125*, 4451.
[18] I. Roy, T. Y. Ohulchanskyy, D. J. Bharali, H. E. Pudavar, R. A. Mistretta, N. Kaur, P. N. Prasad *Proc. Natl. Acad. Sci. USA* **2005**, *102*, 279.
[19] J. Kirstein, B. Platschek, C. Jung, R. Brown, T. Bein, C. Bräuchle *Nat. Mater.* **2007**, *6*, 303.
[20] H. W. Hillhouse, J. W. van Egmond, M. Tsapatsis, J. C. Hanson, J. Z. Larese *Chem. Mater.* **2000**, *12*, 2888.
[21] D. Grosso, C. Boissière, B. Smarsly, T. Brezesinski, N. Pinna, P. A. Albouy, H. Amenitsch, M. Antonietti, C. Sanchez *Nat. Mater.* **2004**, *3*, 787.
[22] S. Tanaka, H. W. Hillhouse, *Chem. Lett.* **2006**, *928.*
[23] O. Terasaki, T. Ohsuna, in *Handbook of Zeolite Science and Technology*, (Eds: S. M. Auerbach, K. A. Carrado, P. K. Dutta), Marcel Dekker, New York **2003**, pp. 291–315.
[24] Y. Sakamoto, M. Kaneda, O. Terasaki, Ø. Y. Zhao, J. M. Kim, G. Stucky, H. J. Shin, R. Ryoo *Nature* **2000**, *408*, 449.
[25] Y. Sakamoto, T. W. Kim, R. Ryoo, O. Terasaki, *Angew. Chem. Int. Ed.* **2004**, *43*, 5231.
[26] V. Kukla, J. Kornatowski, D. Demuth, I. Gimus, H. Pfeifer, L. V. C. Rees, S. Schunk, K. K. Unger, J. Karger *Science* **1996**, *272*, 702.
[27] N. E. Benes, H. Jobic, H. Verweij, *Microporous Mesoporous Mater.* **2001**, *43*, 147.
[28] H. K. M. Tanaka, T. Kurihara, A. P. Mills, Jr., *Phys. Rev. B* **2005**, *72*, 193408.
[29] H. K. M. Tanaka, T. Kurihara, N. Nishiyama, T. Maruo, A. P. Mills, Jr., *Microporous Mesoporous Mater.* **2006**, *95*, 164.
[30] H. K. M. Tanaka, T. Kurihara, A. P. Mills, Jr., *J. Phys. Condens. Matter* **2006**, *18*, 8581.
[31] J. Wawryszczuk, J. Goworek, R. Zaleski, T. Goworek, *Langmuir* **2003**, *19*, 2599.
[32] H. Y. Zhang, Y. J. He, Y. B. Chen, H. Y. Wang, *J. Appl. Phys.* **2002**, *92*, 7636.
[33] Y. J. He, H. Y. Zhang, Y. B. Chen, H. Y. Wang, T. Horiuchi, *J. Phys. Condens. Matter* **2001**, *13*, 2467.
[34] M. P. Petkov, M. H. Weber, K. G. Lynn, K.P. Rodbell, *Appl. Phys. Lett.* **2000**, *77*, 2470.
[35] C. Q. He, M. Muramatsu, T. Ohdaira, A. Kinomura, R. Suzuki, K. Ito and Y. Kobayashi, *Appl. Surf. Sci.* **2006**, *252*, 3221.
[36] Y. Yamauchi, M. Sawada, A. Sugiyama, T. Osaka, Y. Sakka, K. Kuroda, *J. Mater. Chem.* **2006**, *16*, 3693.
[37] H. W. Hillhouse, J.W. van Egmond, M. Tsapatsis, J.C. Hanson and J.Z. Larese, *Microporous Mesoporous Mater.* **2001**, *44*, 639.
[38] Y. Yamauchi, M. Sawada, T. Noma, H. Ito, S. Furumi, Y. Sakka, K. Kuroda, *J. Mater. Chem.* **2005**, *15*, 1137.
[39] C. W. Wu, Y. Yamauchi, T. Ohsuna, K. Kuroda, *J. Mater. Chem.* **2006**, *16*, 3091.
[40] Y. Yamauchi, M. Sawada, M. Komatsu, A. Sugiyama, T. Osaka, N. Hirota, Y. Sakka, K. Kuroda, *Chem. Asian J.*, **2007**, 2, 1505.
[41] R. Ryoo, C. H. Ko, M. Kruk, V. Antochshuk and M. Jaroniec, *J. Phys. Chem. B* **2000**, *104*, 11465.
[42] T. Kurihara, A. Shirakawa, A. Enomoto, T. Shidara, H. Kobayashi, and K. Nakahara, *Appl. Surf. Sci.* **1995**, *85*, 178.
[43] K. Ito, H. Nakanishi, Y. Ujihira, *J. Phys. Chem. B* **1999**, *103*, 4555.
[44] P. Sferlazzo, S. Berko, K. F. Canter, *Phys. Rev. B* **1987**, *35*, 5315.
[45] M. J. Saxton, K. Jacobson, *Annu. Rev. Biophys. Biomol. Struct.* **1997**, *26*, 373.
[46] A. Einstein, *Ann. Phys.* **1905**, *17*, 549.